



Yellow River Delta Wetland Classification Based on Machine Learning Method Combined with Multi-scale Segmentation Approach

Yirong Li ¹, Delong Kong², Moughal Tauqir ^{3*}, Cheng Feng ⁴, Shawkat Ali ⁵, Hidayat Ullah ⁶

¹⁻³ Remote Sensing Information and Digital Earth Center, College of Computer Science and Technology, Qingdao University, Qingdao 266071, China

⁴ Dalian Maritime University, Dalian, 116026, China

⁵⁻⁶ College of Computer Science and Technology, Qingdao University, Qingdao 266071, China

*Corresponding Author: Moughal Tauqir

Article Info

P-ISSN:3051-3383

E-ISSN:3051-3391

Volume: 06

Issue: 02

July - December 2025

Received: 25-09-2025

Accepted: 27-10-2025

Published: 22-11-2025

Page No: 155-163

Abstract

The wetlands of the Yellow River Delta (YRD) are from a coastal wetland ecosystem that is influenced by both ocean tidal dynamics and the substantial sediment deposits carried by the Yellow River. Therefore, accurately classifying the coastal wetlands in the YRD is essential for their utilization, development and the protection of wetland resources. In this study, by using the sentinel-2 multispectral imagery data, we employ machine learning approach integrated with multi-scale segmentation to improve the accuracy of wetland classification in the YRD. The optimal segmentation scale was determined using the ESP2 tool, with spatial units generated based on a shape and compactness factor. Three machine algorithms—Random Forest (RF), K-Nearest Neighbors (KNN), and Support Vector Machine (SVM)—and combining with multi-scale segmentation method were evaluated for their classification performance at the spatial-unit level, with an emphasis on analyzing interactions between feature space and segmentation units. The results demonstrate that multi-scale segmentation integrated with machine learning algorithms significantly enhances classification accuracy, confirming its suitability for heterogeneous wetland landscapes classification.

DOI: <https://doi.org/10.54660/IJAIET.2025.6.2.155-163>

Keywords: Wetland Classification, Machine Learning, Multi-Scale Segmentation, Remote Sensing.

1.Introduction

Wetland ecosystems are among the most vital ecosystem types on Earth, serving as a essential buffer zone between terrestrial and aquatic environment. Beyond supporting rich biodiversity, wetlands provide critical habitats for human development (Liu *et al.*, 2014) ^[18] and play an irreplaceable role in nitrogen absorption, geochemical cycling, and climate regulation (Boesch, 1994) ^[2]. Closely linked to human societal progress, wetlands are fundamental to human health, safety, and sustainable development. They supply critical freshwater resources and serve as habitats for numerous rare species. Additionally, wetlands also improve water quality, mitigate natural disasters such as floods and droughts, restore groundwater reserves, and enhance the productivity of agriculture, forestry, and fisheries.

Wetlands also play an indispensable role in mitigating the global greenhouse effect. Although they occupy only 6.4% of the Earth's land surface, wetlands contain approximately 35% of the carbon stored in the terrestrial biosphere, making them essential components of global carbon cycling. Over the past century, coastal wetlands worldwide have faced increasing pressures, suffering severe losses in ecological integrity and ecosystem services (Seto *et al.*, 2013) ^[20]. Due to human activities and climate change, nearly half of the world's wetlands have disappeared (Davidson, 2014) ^[6]. Since the 1980s, China's wetlands have experienced significant reduction in both area and ecological function (Zhang *et al.*, 2019) ^[32].

These trends are ongoing, leading to serious environmental challenges, particularly within coastal wetland systems, which have become some of the most vulnerable ecosystems globally.

The Yellow River Delta (YRD), formed by the transport and deposition of massive sediments loads delivered by the Yellow River, is China's largest estuarine delta and one of the most dynamic zones of land-sea interaction among major river deltas (Liu *et al.*, 2017) [17]. The convergence of the Yellow River with adjacent marine waters has created the extensive wetland landscape of the YRD. In recent decades, human activities including infrastructure constructions (Qin *et al.*, 2011) [19], tidal flat reclamation (Chen *et al.*, 2011) [4], oil extraction (Chen *et al.*, 2012) [5], and tourism development (Ding *et al.*, 2016) [7] have significantly impacted the wetland ecosystem, leading to increasingly fragile ecological conditions and widespread public concern (Zong *et al.*, 2009) [36]. Given its high ecological activity and critical environmental functions, the conservation of wetland resources in the YRD has received considerably scholarly attention. Existing research reveals that the degradation of Yellow River Delta wetlands has triggered multiple environmental issues, posing severe threats to the area's sustainable economic development (Yang *et al.*, 2018) [29].

Due to its critical role in wildlife conservation, energy production, and agriculture, the YRD has attracted the attention of researchers (Yan *et al.*, 2017) [27]. The YRD wetlands are the largest and youngest coastal wetland ecosystem in China, providing habitats and migration sites for millions of wild birds, as well as spawning and breeding grounds for numerous freshwater and marine species, making the YRD wetlands an ecological barrier in inland regions (Han *et al.*, 2014) [10]. The YRD provides significant ecosystem services, including nutrient cycling, carbon sequestration, and tourism and recreational value. China's second-largest oilfield, the Shengli Oilfield, is located in the YRD wetland area. Energy production and related industrial activities have had a substantial impact on the region's surface and subsurface environments (Tao, 2000) [22]. Currently, agricultural production occupies a large portion of the newly formed deltaic land, relying heavily on freshwater resources from rivers and groundwater. However, activities such as farmland reclamation and coastal land expansion have caused further degradation of wetland resources (Li, 2015) [13]. As a result of intensified human activities and natural geomorphic evolution, the YRD is experiencing increasingly high risk of ecological degradation.

Before the advancement of remote sensing technologies, wetland exploration relied primarily on traditional field-based methods. These conventional approaches were time-consuming, costly, and often caused unintended damage to wetland ecosystems, hindering the development of comprehensive wetland databases (Zhao *et al.*, 2016) [34]. The maturation of remote sensing technology has revolutionized wetland research. With advantages such as extensive spatial coverage, real-time monitoring capabilities, rapid response, and short revisit cycles, remote sensing has been widely applied in large-scale wetland identification, landscape pattern analysis, and dynamic change detection (Yu *et al.*, 2010) [31]. Satellite remote sensing provides continuous spatial surface imagery data, serving as a vital tool for monitoring wetland dynamics. Its ability to capture large-scale, up-to-date wetland information through repeated

observations makes it particularly valuable for obtaining satellite data at regional and even global scales (Jin *et al.*, 2017) [12].

In wetland classification studies, traditional methods have relied heavily on manual interpretation, which is inefficient and prone to subjective bias (Lin *et al.*, 2023) [15]. With rapid advancements of machine learning (ML), researchers increasingly utilized supervised and unsupervised learning techniques to achieve automated wetland classification. Commonly used machine learning algorithms for wetland classification include Support Vector Machines (SVM), Random Forests (RF), and Decision Trees (Sofinskaya *et al.*, 2025) [21]. These methods distinguish wetland types by extracting spectral, textural, and spatial features from remote sensing images and integrating them with classifier training. The widely used RF algorithm effectively handles high-dimensional data and reduces overfitting through ensemble voting, demonstrating high robustness in medium-resolution wetland classification tasks (Li *et al.*, 2018) [14]. However, machine learning-based wetland classification methods still face significant challenges. On one hand, the performance of machine learning algorithms is highly dependent on the quality of manual feature engineering, while the coexistence of heterogeneity and homogeneity in the Yellow River Delta wetlands makes traditional feature extraction inadequate for comprehensively representing complex landform information (Lin *et al.*, 2021) [16]. On the other hand, when processing large-scale remote sensing data, machine learning models incur substantial computational costs with limited improvement in classification accuracy. Studies indicate that traditional machine learning algorithms exhibit significantly increased classification errors in regions with ambiguous wetland boundaries or mixed land cover types (Zhu *et al.*, 2017) [35]. Furthermore, in multi-temporal and multi-source remote sensing data fusion analysis, machine learning methods demonstrate limited effectiveness in capturing the underlying patterns of wetland dynamics. While machine learning algorithms have certain limitations in wetland classification, they still hold advantages in specific scenarios. For instance, Support Vector Machines (SVM) effectively handle nonlinear classification problems, while lightweight decision tree algorithms prove valuable in resource-constrained environments, enabling machine learning methods to address small-scale wetland classification challenges. Therefore, machine learning approaches can provide preliminary classification solutions for wetland research, but further breakthroughs are required for more complex wetland environments.

2. Study Area and Data

2.1. Study area

The Yellow River Delta (YRD) is located between east longitude 117°31'-119°18' and north latitude 36°55'-38°16', mainly distributed in the northeastern part of Shandong Province, adjacent to the Bohai Bay and Laizhou Bay to the north and east respectively (Zhang *et al.*, 2021) [33]. It belongs to the warm temperate semi-humid continental monsoon climate zone, with distinct seasons, sufficient sunlight, and concurrent rainfall and heat. The climate is characterized to mild and temperate monsoon climate (Jiang *et al.*, 2005) [11]. It is relatively humid in summer and dry in winter, with clear seasonality. In this work, the study region is presented in Figure 1.

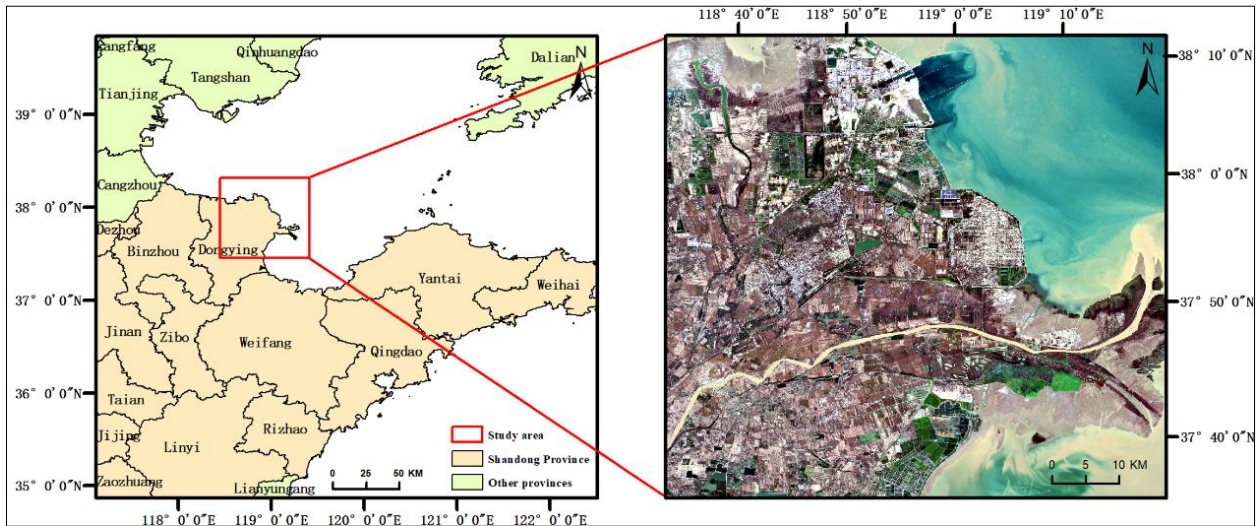


Fig 1: Study region with Sentinel-2 satellite 3-channels color composition image

2.2. Data Source and Preprocessing

Sentinel-2 satellite remote sensing data is widely used for terrestrial and ocean monitoring (Drusch *et al.*, 2012) [8]. Sentinel-2 images combine high spatial resolution, a short-replay period and a rich-spectral range (Xu and Su, 2023) [26], which is highly useful for monitoring the status of land ecosystem, environmental conditions and various vegetation types (Tian and Chen, 2019) [23]. In this work, the Sentinel-2 Level-2A level multispectral data from October 29, 2019 were adopted under low-cloud conditions. The feature information of the Sentinel-2 multispectral data is presented in Table 1, and relevant spectral bands are illustrated in Table 2. Four views of L2A-level Sentinel-2A data from October 29 were used, with less than 1% cloud cover, and all data were atmospherically corrected.

3. Method

3.1. Classification of YRD Wetland Based on Random Forest

Random Forest (RF) is a supervised classification algorithm based on ensemble learning, proposed by Breiman (2001) [3]. It constructs multiple decision trees and employs a majority voting mechanism to complete classification tasks. The method generates multiple training subsets through Bootstrap sampling, with each subset. Its core mechanism includes two types of randomness: 1) Random sampling: This approach employs a self-sampling method to draw samples with replacement from the dataset. Selected samples from the subset for each tree, while unselected ones are used for model validation. This randomness reduces the model's reliance on any single data distribution by generating diverse subsets. 2) Random feature selection: During node splitting in each tree,

$$\text{Gini}(h) = 1 - \sum_{j=1}^k p_j^2(h) \quad (1)$$

where, $p_j^2(h)$ denotes the probability of the j-th category belonging to the training samples, $n(h)$ represents the sample count, and k indicates the number of categories. This mechanism not only reduces inter-tree correlations but also enhances the model's adaptability to high-dimensional data through diversified feature space exploration.

This study employed stratified random sampling to allocate the dataset into a training set (70%) and a test set (30%). Cross-validation was implemented to ensure balanced class distribution and reduce data bias in minority wetland types. During model construction, the random forest parameters were set to 150 trees, a maximum depth of 8 layers, and a Bootstrap feature sampling strategy to enhance model robustness. The Hyperparameter optimization used a stochastic search algorithm, and parallel computing accelerated the training process. Overfitting was monitored using training curves and confusion matrices. The model's generalization ability was evaluated using the Kappa coefficient and overall assessment (OA).

3.2. Wetland Classification of YRD Based on KNN

K-Nearest Neighbors (KNN) algorithm is a non-parametric, instance-based classification method. The idea of this algorithm is that the neighboring samples in the feature space tend to have similar category attributes (Alizadeh and Nikoo, 2018; Wilson *et al.*, 2018) [1, 25]

1. Distance Metrics: Sample similarity is measured using Euclidean distance, Manhattan distance, or cosine similarity. The selection of distance metrics should be based on relevant data characteristics. For instance, cosine similarity is suitable for sparse text features, while Manhattan distance demonstrates greater robustness to outliers. In this study, Euclidean distance is adopted as the measurement metric, with the calculation formula as follows:

$$L(x_i, x_j) = \left(\sum_{l=1}^n |x_i^{(l)} - x_j^{(l)}|^2 \right)^{\frac{1}{2}} \quad (2)$$

where, $x_i = (x_i^1, x_i^2, \dots, x_i^n)$, $x_j = (x_j^1, x_j^2, \dots, x_j^n)$

2. Neighbors Selection: The system selects the nearest K samples to determine predictions through majority voting or weighted averaging, where weights are inversely proportional to distances. This mechanism captures local neighborhood patterns but is sensitive to K-value selection, requiring cross-validation to balance noise sensitivity and generalization.

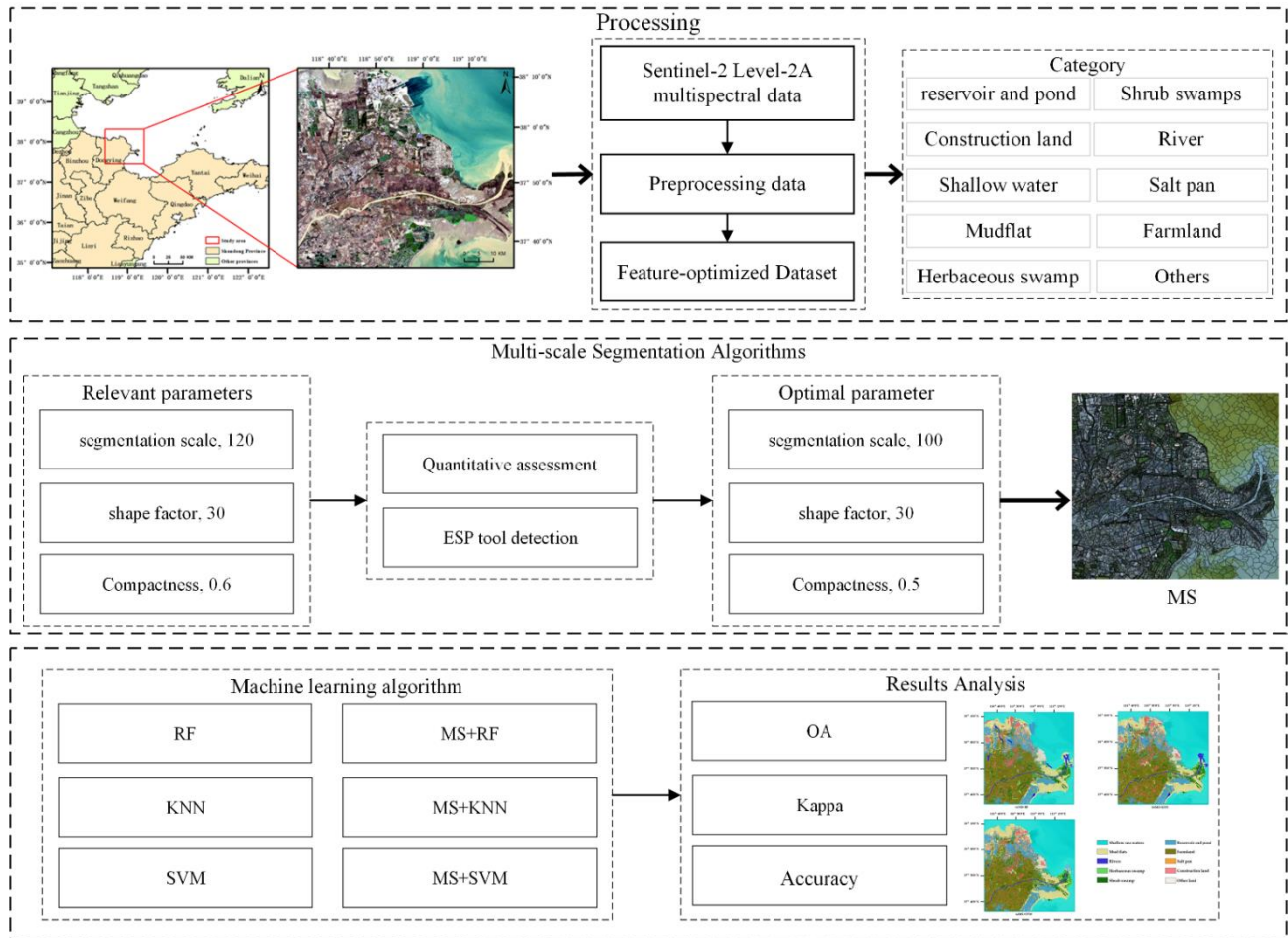


Fig 2: Workflow of this study

Table 1: Levels and product information of Sentinel-2 data

Product Level	Product Introduction
Level-0	raw data
Level-1A	Geometric coarse correction products containing meta-information
Level-1B	Radiance product, embedded in a GCP-optimized geometric model but without the corresponding geometric corrections
Level-1C	Atmospheric Apparent Reflectance Products After Orthorectification and Sub-Image-Level Geometric Refinement Corrections
Level-2A	Contains primarily atmospherically corrected bottom-of-the-atmosphere reflectance data

3. Parameter Optimization: When the K value is too small, it becomes overly sensitive to local noise, which may overlook the local characteristics of the data. Typically, the optimal value is determined through grid search combined with cross-validation.

The standardization is performed to eliminate the influence of band difference on distance calculation. The optimal parameters are determined by grid search and 5-fold cross-validation. The L1 norm is selected as the measurement criterion, and the distance weighted strategy was applied. This configuration can effectively alleviate the classifications.

3.3. Classification of the YRD Wetland Based on SVM

Support Vector Machine (SVM) is a statistical learning algorithm for binary classification (Geiß *et al.*, 2019) [9]. The

idea of SVM is to find the optimal hyperplane of the class intervals.

1. Kernel Techniques: The nonlinear mapping mechanism based on kernel methods resolves the linearly inseparable problem in low-dimensional space through implicit high-dimensional projection. This approach not only avoids explicit high-dimensional computations but also significantly enhances the model's ability to fit complex data distributions.

2. Soft interval optimization: The soft interval support vector machine constructs a structural risk minimization model by introducing slack variables and regularization coefficients, which allows some training samples to not satisfy the strict interval constraint while maintaining the principle of maximum interval classification.

Table 2: Multi-Spectral bands of Sentinel-2 sensor

Band number	Band name	Sentinel-2A		Sentinel-2B		Resolution (m)	
		Central wavelength (nm)	Bandwidth (nm)	Central wavelength (nm)	Bandwidth (nm)		
MSI	1	Coastal aerosol	443.9	20	442.3	20	60
	2	Blue	496.6	65	492.1	65	10
	3	Green	560.0	35	559	35	10
	4	Red	664.5	30	665	30	10
	5	Vegetation Red Edge	703.9	15	703.8	15	20
	6	Vegetation Red Edge	740.2	15	739.1	15	20
	7	Vegetation Red Edge	782.5	20	779.7	20	20
	8	NIR	835.1	115	833	115	10
	8b	Narrow NIR	864.8	20	864	20	20
	9	Water vapour	945.0	20	943.2	20	60
	10	SWIR-Cirrus	1373.5	30	1376.9	30	60
	11	SWIR	1613.7	90	1610.4	90	20
12	SWIR	2202.4	180	2185.7	180	20	



Fig 3: Multi-scale segmentation t results

3. Dual problem solving: The original convex quadratic programming problem is transformed into a dual optimization problem which only involves inner product operation. The solution to this dual problem is uniquely determined by the support vector, and the sparsity mechanism significantly reduces the computational dimension by screening out non-critical samples.

This study employs the SVM algorithm to construct a wetland classification model, systematically addressing the challenges of high-dimensional feature spaces and class imbalance. The methodology involves two key approaches: First, standardizing multidimensional feature data and

dynamically adjusting category penalty weights to mitigate recognition bias in minority class samples such as constructed wetlands. Second, through grid search and 5-fold cross-validation, the study identifies the radial basis function (RBF) kernel as the optimal kernel function, whose nonlinear mapping capability effectively deciphers the complex coupling relationships between wetland spectral and textural features. Compared with KNN and random forest, SVM demonstrates unique advantages in support vector sparsity and high-dimensional nonlinear separability, particularly suitable for fine-grained classification of wetland scenarios with small samples, providing a highly robust solution for dynamic monitoring of wetland ecosystems.

3.4. YRD Classification Based on Multi-scale Segmentation combined Machine Learning

Machine learning-based classification is susceptible to salt-

and-pepper noise, a common image noise type. Object-oriented image analysis methods are the mainstream solution, with image segmentation as its foundation.

Table 3: Classification accuracy for the YRD wetland

Method	OA	Kappa	Accuracy	Classification									
				Shallow water	Mudflat	River	Herbaceous swamp	Shrub swamps	reservoir and pond	Farmland	Salt pan	Construction land	Others
RF	87.20	83.51	PA	82.02	85.06	86.02	65.10	87.39	81.00	88.53	89.41	90.80	82.69
			UA	92.02	92.22	91.36	66.90	80.02	81.06	92.76	91.06	91.41	93.18
MS+RF	90.02	86.57	PA	86.20	86.40	86.68	69.15	89.27	80.90	90.53	94.44	91.80	88.67
			UA	93.82	93.79	92.74	66.97	83.79	85.00	93.78	96.90	94.74	94.25
KNN	83.56	82.11	PA	81.36	83.90	82.50	80.03	70.21	84.30	83.99	75.26	94.34	90.08
			UA	85.20	84.66	83.45	85.01	84.11	90.36	82.68	81.60	83.17	81.95
MS+KNN	86.64	83.98	PA	84.95	82.92	83.05	82.03	72.16	89.38	84.33	77.81	91.81	90.86
			UA	87.29	88.03	87.19	85.09	85.02	93.06	87.68	88.67	85.15	86.95
SVM	84.31	83.26	PA	80.08	83.21	84.25	63.30	88.30	81.00	82.20	90.25	90.01	84.54
			UA	91.29	81.21	83.41	60.19	81.09	82.50	91.00	92.09	90.36	86.56
MS+SVM	87.35	85.36	PA	82.02	85.36	89.33	63.33	85.31	80.69	90.21	93.25	90.54	87.55
			UA	92.28	86.32	85.45	62.28	80.02	84.59	90.55	97.00	90.36	90.22

Multi-scale segmentation enhances data robustness against noise while statistically aggregating features to reduce noise sensitivity. This approach is particularly suitable for high-resolution satellite data. Moreover, it improves data interpretability by correlating regional features (e.g., shape and texture) with ground object attributes, aligning with the requirements of remote sensing applications.

Multi-scale segmentation technology significantly improves the accuracy and interpretability of image classification in complex scenarios by hierarchically analyzing heterogeneous features and spatial contextual semantics (Wang and Jia, 2012) [24]. This approach constructs a hierarchical object network using adaptively optimized scale parameters, capturing fine-scale details while integrating spectral homogeneity and morphological constraints at coarser scales. This methodology effectively addresses the pixel-level classification challenge caused by salt-and-pepper noise and enhances the discrimination capabilities of multi-scale features. Therefore, the classification process combines machine learning with multi-scale segmentation techniques. Object-oriented remote sensing image interpretation requires consideration of the spatial heterogeneity of surface cover. Multi-scale segmentation methods effectively resolve this issue by constructing a hierarchical segmentation-object network (Ye *et al.*, 2025) [30]. Based on regional merging criteria and constrained by heterogeneity thresholds, this approach adaptively generates superpixel objects at different spatial scales. It captures macro-scale geomorphological units through large-scale segmentation while resolving micro-scale feature boundaries via fine-scale segmentation (Yan and Ning, 2008) [28]. For specific interpretation tasks, the method optimizes scale parameters to achieve locally optimal segmentation, providing feature-extraction and classification-ready segmentation primitives suitable for feature-extraction

and classification that align with semantic features.

Within the framework of multi-scale segmentation algorithms, the key control parameters include scale parameters, shape weight coefficients, and compactness weight coefficients. Traditional parameter optimization methods, which rely on manual iterative adjustments and visual evaluation, introduce significant subjective biases and efficiency limitations. To address this, an automated evaluation tool (ESP2) based on global heterogeneity measurement was developed. By constructing local variance rate curves and applying information entropy criteria, the tool quantitatively identifies the balance point between homogeneity within segmented objects and heterogeneity between adjacent objects, thereby achieving adaptive optimization of scale parameters optimization.

The ESP2 tool is built on a fractal network evolution algorithm framework, quantitatively selecting optimal segmentation scales by constructing multi-scale heterogeneity measurement curves. Its core algorithm calculates local variance indices representing homogeneity within image objects at different segmentation scales, then derives change rate curves using first-order derivatives of the LV curve. When the ROC curve exhibits a significant peak, it indicates that rate of the homogeneity enhancement on the image object reaches a critical inflection point at the corresponding segmentation scale, which corresponds to the optimal granularity for the specific land feature categories.

$$ROC = (L_{i+1} - L_i) / L_i \times 100\% \quad (3)$$

where L_i is the average standard deviation of the i -th layer object; L_{i+1} is the average standard deviation of the $(i+1)$ -th layer object.

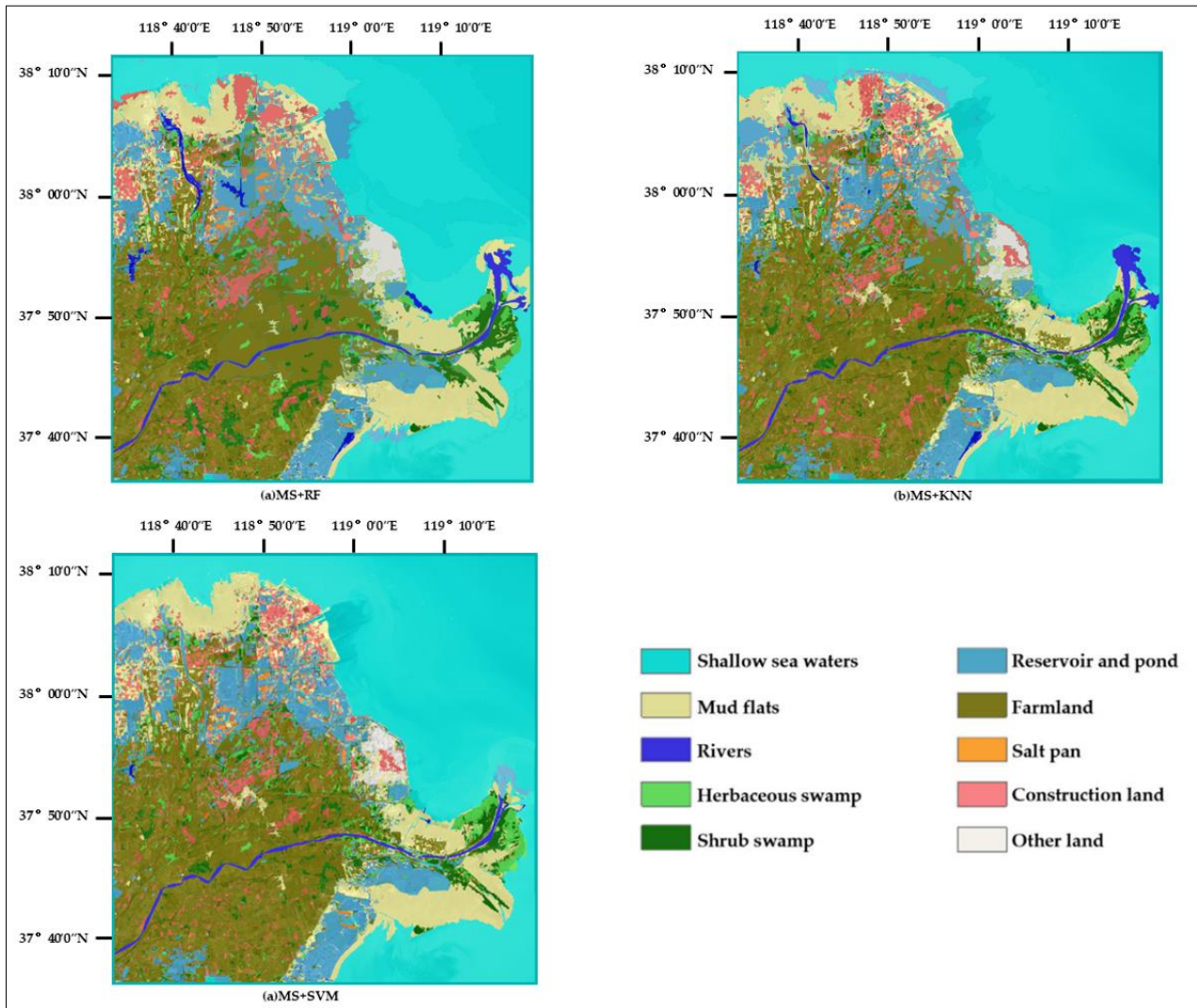


Fig 4: Classification of YRD wetland based on three models combined with multi-scale segmentation

This study employs a multi-scale segmentation parameter dynamic optimization method, as illustrated in Figure 2. The process begins with initial segmentation using preset parameters (segmentation scale=120, shape factor=30, compactness=0.6) on a feature-optimized dataset, generating basic semantic object primitives.

The object feature vector was constructed using 26 features, including spectral mean, texture variance, and vegetation index. Objects were classified using a Random Forest classifier. This method effectively suppresses pixel-level salt-and-pepper noise by homogenizing object-level features. Figure 3 displays the object boundaries (black outlines) generated using the optimized segmentation parameters.

4. Results

4.1. YRD Classification Results based on Multi-scale Segmentation and Machine Learning

As shown in Table 3, this study demonstrates the classification accuracy of multi-scale segmentation combined with machine learning algorithms for the YRD wetlands. The table compares the performance metrics of three methods: Random Forest (RF), Support Vector Machine (SVM), and K-Nearest Neighbors (KNN). The experimental results reveal significant differences in performance across 10 land object categories, with Random Forest showing relative superiority

in wetland type classification. These findings validate the feasibility of integrating multi-scale segmentation with machine learning, providing empirical evidence for selecting appropriate wetland classification methods.

Table 3 shows that Random Forest (RF) achieves the best overall performance. When combined with the multi-scale segmentation algorithm, it achieves an overall accuracy of 90.02% and a Kappa coefficient of 86.57, with its majority class accuracy outperforming other methods. In Salt pan classification, RF achieves producer accuracy of 94.44% and a user accuracy of 96.90%, while both producer accuracy (PA) and user accuracy (UA) for construction land both exceed 90%. However, RF shows weaker performance in herbaceous swamp classification, with significantly missed classifications.

The KNN model combining multi-scale segmentation achieved an overall accuracy of 86.64% and a Kappa coefficient of 83.98, slightly inferior to Random Forest (RF) but demonstrating strong performance in specific categories. For instance, it classified herbaceous wetlands with PA/UA values of 82.03% and 85.09%, while reservoirs with a UA accuracy of 93.06%—significantly outperforming both RF and Support Vector Machines (SVM). However, KNN showed limited accuracy in Salt pan and Shrub swamps wetlands, and its construction land with UA accuracy

dropping to 85.15%, indicating its limited ability to process high-dimensional features and nonlinear relationships.

The SVM model combined with multi-scale segmentation achieved an overall accuracy (OA) of 87.35% and a Kappa coefficient of 85.36. Its UA classification for Salt pan reached the highest accuracy of 97.00%, outperforming both Random Forest (RF) and K-Nearest Neighbors (KNN). However, the classification accuracy for herbaceous and shrub swamp categories was significantly lower. In farmland classification, SVM demonstrated stable performance comparable to RF, although its generalization ability for complex land features was slightly inferior to RF.

Figure 4 presents the classification performance of various algorithms integrated with multi-scale segmentation. Random Forest demonstrates high accuracy and robustness across most categories, particularly excelling in clearly defined land features such as salt pans and construction sites. KNN performs well for categories in tasks with distinct local features such as herbaceous marshes and reservoirs, though its overall stability is limited. SVM shows slight superiority in the User's Accuracy (UA) of salt pans but remains sensitive to categories with ambiguous boundaries, requiring further optimization of kernel functions and parameters. Experimental results indicate that incorporating machine learning with multi-scale segmentation algorithms enhances classification accuracy for all machine learning approaches to varying degrees.

5. Conclusion

In this study, we applied three machine learning algorithms—random forest, K-nearest neighbors, and support vector machines (SVM) and integrated with multi-scale segmentation algorithms for classification of YRD wetland. Experimental results demonstrated that the random forest (RF) algorithm achieves significantly higher overall accuracy than SVM and KNN, particularly excelling in salt marsh and construction land classification. However, RF shows relatively lower Producer's Accuracy (PA) for herbaceous swamps producers, indicating spectral confusion between these wetland types and farmland. Furthermore, after optimizing object boundaries through multi-scale segmentation, the misclassification between farmland and marsh is effectively reduced, validating the method's applicability in high-heterogeneity wetland classification.

The study results indicated that the machine learning algorithm incorporating multi-scale segmentation significantly improved overall accuracy and enhanced terrain boundary recognition in high-resolution imagery compared to the original method. By optimizing object boundaries through multi-scale segmentation, the misclassification between farmland and wetlands is effectively mitigated, validating the approach's adaptability to highly heterogeneous wetland boundaries. Further analysis reveals that the classification model based on object-level spectral, textural, and geometric features not only improves overall classification precision but also markedly enhances terrain boundary identification in high-resolution imagery, outperforming conventional methods.

Research further demonstrates that multiscale segmentation, by optimizing spatial object boundaries, effectively reduces morphological confusion between heterogeneous objects, thereby minimizing classification errors in high-resolution wetland habitats. The method's applicability in highly

heterogeneous wetlands has been validated. Consequently, the classification model integrating object-level spectral-textural-geometric features achieves higher overall accuracy compared with the traditional pixel-based approaches while reducing boundary fitting errors in high-resolution imagery.

6. Acknowledgments

This work was supported by Shandong Provincial Natural Science Foundation (No. ZR2020GF067, ZR2024LQX005).

Author Contributions

Yirong Li: data curation, investigation, software, methodology, formal analysis, writing—original draft preparation. Delong Kong: formal analysis, investigation, validation, writing—review and editing. Moughal Tauqir: Funding acquisition, Project administration, writing—review and editing. Cheng Feng: formal analysis, investigation. Shawkat Ali: writing—review and editing. Hidayat Ullah: writing—review and editing. Yirong Li and Delong Kong contributed equally to this work All authors have read and agreed to the published version of the manuscript.

Declaration of competing interest

The authors declare that they have no known competing financial interests or personal relationships that could have appeared to influence the work reported in this paper.

7. References

1. Alizadeh MR, Nikoo MR. A fusion-based methodology for meteorological drought estimation using remote sensing data. *Remote Sens Environ.* 2018;211:229-47. doi:10.1016/j.rse.2018.04.001
2. Boesch DF. Scientific assessment of coastal wetland loss, restoration and management in Louisiana. Fort Lauderdale (FL): Coastal Education and Research Foundation; 1994.
3. Breiman L. Random forests. *Mach Learn.* 2001;45(1):5-32. doi:10.1023/A:1010933404324
4. Chen J, Wang S, Mao Z. Monitoring wetland changes in Yellow River Delta by remote sensing during 1976-2008. *Prog Geogr.* 2011;30(5):585-92. Chinese.
5. Chen K, Xiao N, Wang B, Li J. The effects of petroleum exploitation on water quality bio-assessment and benthic macro-invertebrate communities in the Yellow River Delta wetland. *Acta Ecol Sin.* 2012;32(6):1970-8. Chinese.
6. Davidson NC. How much wetland has the world lost? Long-term and recent trends in global wetland area. *Mar Freshw Res.* 2014;65(10):934-41. doi:10.1071/MF14173
7. Ding T, Zhou T, Zhu X, Yang Y. On dynamic changes of wetland in Yellow River Delta with remote sensing images. *J Southwest China Norm Univ (Nat Sci Ed).* 2016;41(4):52-7. doi:10.13718/j.cnki.xsxb.2016.04.011. Chinese.
8. Drusch M, Del Bello U, Carlier S, Colin O, Fernandez V, Gascon F, *et al.* Sentinel-2: ESA's optical high-resolution mission for GMES operational services. *Remote Sens Environ.* 2012;120:25-36. doi:10.1016/j.rse.2011.11.026
9. Geiß C, Aravena Pelizari P, Blickensdörfer L, Taubenböck H. Virtual support vector machines with self-learning strategy for classification of multispectral remote sensing imagery. *ISPRS J Photogramm Remote Sens.* 2019;151:42-58. doi:10.1016/j.isprsjprs.2019.03.001
10. Han G, Xing Q, Yu J, Luo Y, Li D, Yang L, *et al.* Agricultural reclamation effects on ecosystem CO₂ exchange of a coastal wetland in the Yellow River Delta. *Agric Ecosyst Environ.* 2014;196:187-98.

- doi:10.1016/j.agee.2013.09.012
11. Jiang W, Li J, Wang W, Xie Z, Mai S. Assessment of wetland ecosystem health based on RS and GIS in Liaohe River delta. In: Proceedings. 2005 IEEE International Geoscience and Remote Sensing Symposium; 2005 Jul 25-29; Seoul, Korea (South). Piscataway (NJ): IEEE; 2005. p. 2384-6. doi:10.1109/IGARSS.2005.1525457
 12. Jin H, Huang C, Lang MW, Yeo IY, Stehman SV. Monitoring of wetland inundation dynamics in the Delmarva Peninsula using Landsat time-series imagery from 1985 to 2011. *Remote Sens Environ*. 2017;190:26-41. doi:10.1016/j.rse.2016.12.001
 13. Li J. Study of building the ecological compensation system of wetland in Shandong Yellow River Delta. *For Sci Technol*. 2015;40(4):52-5. Chinese.
 14. Li Y, Zhang H, Xue X, Jiang Y, Shen Q. Deep learning for remote sensing image classification: a survey. *WIREs Data Mining Knowl Discov*. 2018;8(6):e1264. doi:10.1002/widm.1264
 15. Lin X, Cheng Y, Chen G, Chen W, Chen R, Gao D, *et al*. Semantic segmentation of China's coastal wetlands based on Sentinel-2 and Segformer. *Remote Sens*. 2023;15(15):3714. doi:10.3390/rs15153714
 16. Lin Z, Wang J, Li W, Jiang X, Zhu W, Ma Y, *et al*. OBH-RSI: object-based hierarchical classification using remote sensing indices for coastal wetland. *J Beijing Inst Technol*. 2021;30(2):159-71. doi:10.15918/j.jbit1004-0579.2021.014
 17. Liu D, Li Y, Wang Z, Yang Q, Li Y. Dynamic and driving factors of landscape types and landscape pattern in Yellow River Delta from 1983 to 2014. *Shandong For Sci Technol*. 2017;47(1):1-8. Chinese.
 18. Liu G, Zhang L, Zhang Q, Musyimi Z, Jiang Q. Spatio-temporal dynamics of wetland landscape patterns based on remote sensing in Yellow River Delta, China. *Wetlands*. 2014;34(4):787-801. doi:10.1007/s13157-014-0542-1
 19. Qin T, Qi W, Xu B, Shang R, Sun C. Impacts of road on land use based on RV index in Yellow River Delta. *J Hebei Agric Sci*. 2011;15(11):67-72. doi:10.16318/j.cnki.hbnykx.2011.11.003. Chinese.
 20. Seto KC, Parnell S, Elmqvist T. A global outlook on urbanization. In: Elmqvist T, *et al.*, editors. *Urbanization, biodiversity and ecosystem services: challenges and opportunities*. Dordrecht: Springer; 2013. p. 1-12. doi:10.1007/978-94-007-7088-1_1
 21. Sofinskaya OA, Mouraviev FA, Rakonjac D, Mannapova LM. Application of machine learning algorithms to classify soil components with different hydrophilicity. *Eurasian Soil Sci*. 2025;58(1):28-39. doi:10.1134/S1064229324603652
 22. Tao S. Conflict and coordination development of wetland conservation and petroleum production in the Yellow River Delta. *Ecol Nat Prot*. 2000;(6):26-8. doi:10.14026/j.cnki.0253-9705.2000.06.010. Chinese.
 23. Tian Y, Chen Z. ESA Sentinel-2A/B satellite: characteristics and applications. *J Beijing Norm Univ (Nat Sci)*. 2019;55(1):57-64. Chinese.
 24. Wang L, Jia Z. Multi-scale image segmentation algorithm based on support vector machine approximation criteria. *Concurrency Comput Pract Exper*. 2012;24(11):1231-8. doi:10.1002/cpe.1893
 25. Wilson BT, Knight JF, McRoberts RE. Harmonic regression of Landsat time series for modeling attributes from national forest inventory data. *ISPRS J Photogramm Remote Sens*. 2018;137:29-46. doi:10.1016/j.isprsjprs.2018.01.006
 26. Xu L, Su T. The method of algal bloom extraction in Lake Chaohu waters based on FAI-L method. *J Lake Sci*. 2023;35(4):1222-33. doi:10.18307/2023.0416. Chinese.
 27. Yan F, Liu X, Chen J, Yu L, Yang C, Chang L, *et al*. China's wetland databases based on remote sensing technology. *Chin Geogr Sci*. 2017;27(3):374-88. doi:10.1007/s11769-017-0872-z
 28. Yan G, Shu NH. Binary MRF model and multi-scale texture segmentation of multi-band remote sensing image. *Geomat Inf Sci Wuhan Univ*. 2008;33(1):21-4. Chinese.
 29. Yang W, Pei J, Li X, Sun T, Wang W. Effect evaluation and management strategies for freshwater restoration projects in Yellow River Delta wetlands. *J Beijing Norm Univ (Nat Sci)*. 2018;54(1):98-103. doi:10.16360/j.cnki.jbnuns.2018.01.013. Chinese.
 30. Ye Z, Li Y, Li Z, Liu H, Zhang Y, Li W. Attention multiscale network for semantic segmentation of multimodal remote sensing images. *IEEE Trans Geosci Remote Sens*. 2025;63:1-15. doi:10.1109/TGRS.2025.3540848
 31. Yu H, Zhang S, Kong B. Comparison and analysis of wetland cover classification by using CBERS and TM imagery. *Remote Sens Inf*. 2010;(3):75-81. Chinese.
 32. Zhang J, Li J, Lu Y, Xiao L. Current situation, problems and management countermeasures of coastal wetlands in China. *Environ Sustain Dev*. 2019;44(5):127-9. doi:10.19758/j.cnki.issn1673-288x.201905127. Chinese.
 33. Zhang X, He S, Yang Y. Evaluation of wetland ecosystem services value of the Yellow River Delta. *Environ Monit Assess*. 2021;193(6):353. doi:10.1007/s10661-021-09130-x
 34. Zhao X, Han M, Yu W, Liu L, Li G. Research on degradation of the Yellow River Delta wetland based on remote sensing image. *Yellow River*. 2016;38(3):59-64. Chinese.
 35. Zhu XX, Tuia D, Mou L, Xia GS, Zhang L, Xu F, *et al*. Deep learning in remote sensing: a comprehensive review and list of resources. *IEEE Geosci Remote Sens Mag*. 2017;5(4):8-36. doi:10.1109/MGRS.2017.2762307
 36. Zong X, Liu G, Qiao Y, Lin S. Study on dynamic changes of wetland landscape pattern in Yellow River Delta. *J Geo-Inf Sci*. 2009;11(1):91-7. Chinese.

How to Cite This Article

Li Y, Kong D, Tauqir M, Feng C, Ali S, Ullah H. Yellow River Delta wetland classification based on machine learning method combined with multi-scale segmentation approach. *Int J Artif Intell Eng Transform*. 2025;6(2):155-63. doi:10.54660/IJAET.2025.6.2.155-163.

Creative Commons (CC) License

This is an open access journal, and articles are distributed under the terms of the Creative Commons Attribution-NonCommercial-ShareAlike 4.0 International (CC BY-NC-SA 4.0) License, which allows others to remix, tweak, and build upon the work non-commercially, as long as appropriate credit is given and the new creations are licensed under the identical terms.